

# Resolved Near-Infrared Spectroscopy of the Mysterious Pre-Main Sequence Binary System T Tau S

G. Duchêne, A. M. Ghez & C. McCabe

*Division of Astronomy and Astrophysics, UCLA, Los Angeles, CA 90095-1562*

duchene@astro.ucla.edu

## ABSTRACT

We obtained new near-infrared images of the prototypical pre-main sequence triple system T Tau, as well as the first resolved medium-resolution spectra of the close pair T Tau S. At the time of our observations, the tight binary had a 13 AU projected separation and showed significant motion since its discovery, three years before. The orbit cannot be strongly constrained yet, but the observed motion of T Tau Sb with respect to T Tau Sa suggests that the system is at least as massive as T Tau N itself. This may indicate that T Tau N is not the most massive star in the system. The spectrum of T Tau Sa, which is totally featureless except for a strong Br $\gamma$  emission line, identifies this component with the “infrared companion”, whose exact nature remains obscure but may be the consequence of it being the most massive component of the system. Contrasting sharply with T Tau Sa, the spectrum of T Tau Sb shows numerous photospheric features consistent with an early-M spectral type. The presence of a strong Br $\gamma$  emission line and of a significant veiling continuum classifies this object as a deeply embedded T Tauri star. From these observations, we conclude that both components of T Tau S are embedded in their own dense circumstellar cocoon of material, which are probably fed by a much more extended structure.

*Subject headings:* binaries: close — circumstellar matter — stars: pre-main-sequence — stars: individual (T Tau S)

## 1. Introduction

T Tau has long been identified as one of the brightest low-mass pre-main sequence objects and, as such, has been considered as the prototype for the T Tauri class of objects (Joy 1945). Its notable properties include a significant infrared continuum excess thought to

be related to the presence of an accretion disk around this million year-old object (Bertout et al. 1988), a bright nebulosity caused by photon scattering on the inner wall of a cavity emptied by a strong polar outflow (Stapelfeldt et al. 1998), a substantial circumstellar disk resolved through interferometric imaging at radio wavelengths (Akeson et al. 1998) and a limited interstellar extinction ( $A_V \sim 1.5$  mag, Ghez et al. 1991). Early near-infrared high-angular resolution observations revealed a close ( $0''.7$ , or 100 AU at  $d = 140$  pc, Elias 1978) companion in this system (Dyck et al. 1982), which raised the possibility that T Tau is not so prototypical of its class. From subsequent various high-angular resolution surveys (Ghez et al. 1993; Leinert et al. 1993; Simon et al. 1995) however, it rapidly became clear that binarity is not a rare property, re-establishing T Tau as a prototype of pre-main sequence solar-type stars once again.

The companion to T Tau, known as T Tau S, is a very peculiar one. While it is undetected in visible images obtained first by speckle interferometry (Gorham et al. 1992) and more recently by HST/WFPC2 (Stapelfeldt et al. 1998), implying a huge flux ratio at those wavelengths ( $\Delta V > 9.5$ ), its bolometric luminosity is about twice as large as that of T Tau N. Indeed, T Tau S dominates the system flux at wavelengths  $\gtrsim 2 \mu\text{m}$  and its spectral energy distribution peaks around  $3 \mu\text{m}$ , a significantly longer wavelength than normal for T Tauri stars (Ghez et al. 1991). Near- to mid-infrared monitoring has further revealed that T Tau S is strongly variable, up to 2 mag over timescales of a few months (Ghez et al. 1991). Finally, its near-infrared spectrum is featureless around  $2 \mu\text{m}$  at a resolution of  $R \sim 760$ , with the exception of a large  $\text{Br}\gamma$  emission line and a much weaker  $\text{H}_2$  line (Beck et al. 2001). Together with a handful of other companions to T Tauri stars, T Tau S has been classified as an “infrared companion” (IRC). As reviewed by Koresko et al. (1997), the peculiar properties of these companions has generated a wide range of theories regarding their nature, which include an embedded intermediate- to high-mass protostar, a planetary object embedded in the disk surrounding their optical companion or a strongly accreting FU Ori-like object among others possibilities. The very nature of T Tau S and other IRCs is still debated as none of these explanations fit all the observational data.

Increasing the complexity of the T Tau system, Koresko (2000) identified a very close companion to T Tau S through speckle holography. In the discovery images, the companion was projected a mere 7 AU ( $0''.05$ ) away from the IRC. Such a small separation raised new questions about the T Tau S system: are both components classifiable as IRCs? If embedded, are they inside the same cocoon of material? Can the additional companion be used to clarify the nature of IRCs? While previous high-angular resolution observations of this system never resolved the IRC (e.g., Simon et al. 1996), follow-up observations by Köhler et al. (2000) confirmed the presence of a close companion. However, they noted significant changes in the binary separation and position angle, which cannot be accounted for by measurement

uncertainties, but rather suggests that the two objects are bound with an orbital period on the order of 10–20 yrs.

In this paper, we present adaptive optics images obtained with the Keck telescope as well as the first spatially resolved  $K$ -band spectra of the T Tau S system. Our observations and data reduction procedures are described in § 2 and our main results are presented in § 3. Implications on the nature of the IRC and its companion are presented in § 4. Finally, § 5 summarizes our findings.

## 2. Observations

The observations presented in this paper were obtained on 2000 November 19 on the 10 m Keck II telescope with the facility near-infrared spectrometer NIRSPEC (McLean et al. 2000) installed behind the adaptive optics system (Wizinowich et al. 2000). T Tau N ( $R = 9.2$ ) was used as a natural guide star for the adaptive optics system and images of the whole T Tau system, including T Tau N, were obtained using SCAM, the slit-viewing camera, with both  $H^1$  and  $K$  broad-band filters at four dithered positions over the detector to correct for bad pixels and flat-field variations. Total integration times were 40 seconds with both  $H$  and  $K$  filters and we achieved Strehl ratios of 24% at  $H$  and 30% at  $K$ . The resolution of the images, measured as the FWHM of a gaussian fit to the radial profile of the unresolved star T Tau N, are respectively 40 and 50 mas at  $H$  and  $K$ . Both components of T Tau S appear unresolved at these resolutions in our images.

Long slit  $K$ -band medium-resolution spectra of the T Tau S components were obtained by aligning the  $0''.036$ -wide slit along the binary position angle; four spectra were obtained at various locations behind the slit, amounting to a total exposure time of 8 minutes. The spectra extend from  $2.0\ \mu\text{m}$  to  $2.4\ \mu\text{m}$  with a  $4.3\ \text{\AA}/\text{pixel}$  scale and have a spectral resolution of  $R \sim 3500$  as measured from the FWHM of various unresolved arc lines. Arc lamps were observed for wavelength calibration and a halogen lamp image was used for estimating the pixel-to-pixel response of the detector. A spectrum of HR 1388, an A7 dwarf, was obtained with the same set-up immediately before T Tau S at a comparable airmass to correct for the numerous atmospheric absorption lines and bands. To remove the strong  $\text{Br}\gamma$  absorption line for this A-type star, we also observed HD 1520, an F8 star, whose spectra can be compared

---

<sup>1</sup>The filter we used, “NIRSPEC-3”, is a customized filter specific to the instrument. Its central wavelength ( $\lambda_c = 1.625\ \mu\text{m}$ ) and bandwidth ( $\Delta\lambda = 0.36\ \mu\text{m}$ ) are close enough to the standard broadband  $H$  filter ( $\lambda_c = 1.630\ \mu\text{m}$ ,  $\Delta\lambda = 0.31\ \mu\text{m}$ ) that we do not expect magnitudes differences larger than a few hundredths. Throughout our paper, we therefore refer to this filter as the  $H$  filter.

to the well-known solar spectra (G2 spectral type) to isolate telluric absorption lines in the vicinity of the hydrogen line, using the method described by Hanson et al. (1996). We also observed a few late-type stars of known spectral type with the same set-up to be used as templates. These objects are 61 Cyg A, Gl 123 and HD 1326, whose spectral types are K5, M0, and M2 respectively.

All data reduction procedures were performed using IRAF<sup>2</sup> for both imaging and spectroscopic data. Accurate astrometry and relative photometry were extracted by point spread function fitting, using T Tau N as an unresolved source, and the standard deviations between the four dithered positions gave us an estimate of the uncertainties for both filters. The astrometry was then combined with the absolute orientation of the detector on the sky, known to  $\pm 0.1$  or so, and its known plate scale ( $17.2 \pm 0.1$  mas/pixel, D. Le Mignant, priv. comm.). The sharper images at shorter wavelengths, together with the variation of flux ratio with wavelength in the T Tau S system, are such that the binary is more easily resolved in the *H*-band images and, although both filters yielded compatible measurements, the astrometric binary parameters given in this paper were extracted from the *H*-band image only.

The pipeline developed to reduce the spectroscopic data performs the following usual reduction steps: sky subtraction, distortion corrections, flat-fielding, bad pixels and cosmic rays removal. To extract the spectra of both components, a gaussian profile, which represents the core of the stellar profiles very well, was fit to both stars along the spatial direction for each of the 1024 spectral slices of the reduced spectrum; the width of the gaussian was forced to be the same for both stars in that process. A Lorentzian profile, which provides a better fit of the wings of the point spread function, was also used in a separate analysis of the same reduced spectra, but resulted in noisier, though similar, spectra; this is due to the relatively high Strehl ratios in our images, which ensure that most of the flux is contained in the stellar cores. In the following, we thus adopt the spectra extracted using a gaussian profile. We estimate that contamination introduced by the wing of the primary’s point spread function on the spectrum of the secondary amounts to less than 10 % of the latter at any wavelength based on the observed radial profile.

The dominant sources of noise in the final spectra are the gaussian fitting process and the atmospheric absorption correction. Estimates for the signal-to-noise ratios can be obtained by studying line-free sections of the stellar spectra; the signal-to-noise ratio in the final spectra is about 60–80 per pixel<sup>3</sup> for both stars in the spectral range 2.08–2.38  $\mu\text{m}$ . Outside

---

<sup>2</sup>IRAF is distributed by the National Optical Astronomy Observatories, which is operated by the Association of Universities for Research in Astronomy, Inc., under contract to the National Science Foundation

<sup>3</sup>The spectral resolution element is about 50 % larger than the pixel size.

this range, the quality of the spectra drops sharply because of strong atmospheric absorption features, poor filter transmission, and detector response.

### 3. Results

#### 3.1. Astrometry and relative photometry

Our final  $H$ - and  $K$ -band images are presented in Fig. 1, while the astrometry and relative photometry extracted through point spread function fitting are summarized in Table 1. T Tau S is clearly resolved at both wavelengths. To confirm the detection of the two components and to confirm our astrometric and photometric measurements, we applied a light deconvolution process with the Richardson-Lucy algorithm implemented in IRAF. T Tau N was used as an unresolved point spread function and we ran 10 iterations after having re-sampled the images by a factor of two in each direction. The deconvolved images are also shown in Fig. 1. The two components are nicely recovered and the quantitative information presented in Table 1 agree very well with the deconvolved images. The location of T Tau Sb with respect to T Tau Sa, which is significantly different from previous measurements, confirms the relative motion of the two stars reported by Köhler et al. (2000). At the time of our observations, the projected separation of the binary was  $12.9 \pm 0.4$  AU. The nature of the observed motion is discussed in § 4.

The flux ratio between the two components of T Tau S has also changed over the last few years. Koresko (2000) measured  $\Delta K_{Sa-b} = 2.61 \pm 0.24$  in December 1997 and Köhler et al. (2000) found  $\Delta H_{Sa-b} = 1.47 \pm 0.05$  in February 2000, which both differ from our observations by  $\gtrsim 3\sigma$ . In spite of the lack of absolute photometry, the variable source can be deduced from the  $K$ -band datasets. The  $K$ -band flux ratio between T Tau N and T Tau Sa is identical, to within statistical uncertainties, and the  $K$ -band flux of T Tau N has been almost constant over the last ten years (Kobayashi et al. 1994; Beck & Simon 2001). Therefore, we conclude that T Tau Sb is itself variable and brightened between the two epochs while T Tau Sa remained constant. Our measurements also show that T Tau S as a whole was close to its bright state at the time of our observations, since the magnitude difference between T Tau N and the unresolved T Tau S system appears to vary from  $\sim 0.5$  to  $\sim 2.5$  mag (Ghez et al. 1991; Roddier et al. 2000). Furthermore, if T Tau Sa always dominates its companion at  $K$ , the known variability of the unresolved T Tau S system indicates that both components are variable.

### 3.2. T Tau Sa spectrum

The spectrum of T Tau Sa is in general featureless apart from a prominent  $\text{Br}\gamma$  emission line which has an equivalent width of  $3.8 \pm 0.2 \text{ \AA}$  (see Fig. 2 and Table 2). Similar equivalent widths for that line were reported by Herbst et al. (1996) and Beck et al. (2001), although we failed to detect the  $2.12 \mu\text{m}$   $\text{H}_2$  emission line that was detected with an equivalent width of  $3.1 \pm 1.4 \text{ \AA}$  by the latter group; our  $3\sigma$  upper limit on its equivalent width is  $0.5 \text{ \AA}$ . A likely explanation for that discrepancy is that the emission could arise from the gas surrounding the star, as already suggested by Beck et al. (2001); their observations were performed through a  $0''.8$ -slit which is much wider than ours, and the surrounding nebulosity has already been detected in this  $\text{H}_2$  line (van Langevelde, van Dishoeck, van der Werf, & Blake 1994). Otherwise, this line could be strongly variable in T Tau Sa or the previous detection, which is only marginally significant, is spurious.

### 3.3. T Tau Sb spectrum

Several features, including the  $^{12}\text{CO}$  ( $\Delta\nu = 2$ ) bands at  $\sim 2.3 \mu\text{m}$  and beyond and the Na doublet at  $2.2 \mu\text{m}$ , can be detected in the spectrum of T Tau Sb when using HR 1388 as the atmospheric calibrator. However, a slight mismatch in airmass (by about 0.08) between this calibrator and T Tau S and the time dependence of the atmosphere impede a perfect correction. To more accurately remove the telluric features from the spectrum of T Tau Sb, we used the spectrum of T Tau Sa, which was observed simultaneously and was found to be featureless with the exception of  $\text{Br}\gamma$  (see § 3.2). The  $\text{Br}\gamma$  line appears “in emission” in the spectrum of T Tau Sb shown in Fig. 2 because the equivalent width of this line is larger in the spectrum of the secondary, but its actual strength cannot be directly measured from this plot. Therefore, the equivalent width of the hydrogen line of T Tau Sb was extracted from the spectrum using HR 1388 as a calibrator, while the discussion of all other parts of the spectrum refers to that obtained using T Tau Sa as a calibrator. No emission is detected at the wavelength of the  $2.12 \mu\text{m}$   $\text{H}_2$  line, with a  $3\sigma$  upper limit of  $0.5 \text{ \AA}$  for its equivalent width.

The spectrum of T Tau Sb contains a number of significant features that appear in all four individual spectra. Among these, sixteen atomic and molecular features are confidently identified (and labelled in Fig. 2), whose relative strength allow us to estimate the spectral type of T Tau Sb. This can be done by comparing the spectrum we obtained to spectral atlases found in the literature or to the standard stars observed during the same run, which is preferred since the instrumental set-up matches perfectly that used for T Tau S. As can be seen from Fig. 2, the spectrum of T Tau Sb seems very similar to those of the two early-M

stars Gl 123 and HD 1326. The K5 star (61 Cyg A) we also observed shows more and stronger Si and Ti features with comparison to the other spectral lines and does not match well the spectrum of T Tau Sb. The latter shows stronger Al and Mg features at  $\sim 2.11 \mu\text{m}$  than HD 1326 (M2), but a much weaker Mg line at  $2.28 \mu\text{m}$  than Gl 123 (M0). On the other hand, the ratio of the two lines of the Na doublet at  $2.2 \mu\text{m}$  appears very similar in T Tau Sb and Gl 123 while that of HD 1326 is significantly different. Although a very accurate estimate of the spectral type would require a higher signal-to-noise spectrum as well as more spectral type standards, we conclude that T Tau Sb has a spectral type M1 with an uncertainty of about one subclass. A similar comparison of the spectrum of T Tau Sb to spectral atlases in the literature (Kleinman & Hall 1986; Ali et al. 1995; Wallace & Hinkle 1997) suggests a spectral type later than K6 and earlier than M2–M3, consistent with the result presented above.

It is interesting to note that all the features detected in the spectrum of T Tau Sb appear much weaker than in the early-M spectral standards observed at the same resolution. The equivalent width of the strongest features (CO bands, Na doublet, Ca triplet at  $2.26 \mu\text{m}$ , Al line at  $2.117 \mu\text{m}$ ) across the whole *K*-band are indeed  $\sim 3$  times smaller than that of the spectral standards. This is quite unlikely to be the cause of a mismatch in luminosity class, since Kleinman & Hall (1986) have shown that only the CO bands are very sensitive to this parameter. Furthermore, although T Tauri stars are frequently thought of as subgiants, the latter have stronger, and not weaker, CO bands. It thus seems that the spectrum of T Tau Sb contains, in addition to its M1 photospheric component, a roughly flat continuum throughout the  $2.1\text{--}2.35 \mu\text{m}$  range. This *K*-band excess must represent about 200 % of the photospheric flux to account for the observed weakness of the various features. This is much larger than the 10 % upper limit we placed on the contamination from the featureless spectrum of the primary, and we conclude that it is intrinsic to the object.

## 4. Discussion

### 4.1. T Tau Sb : A normal active T Tauri star

The unresolved appearance and the photospheric features in the spectrum of T Tau Sb both point to a stellar nature for this object. Although it cannot be definitely excluded that we are seeing scattered light off a compact, dense dust clump in the environment of T Tau Sa whose intrinsic spectrum would then be that of a M1 dwarf, the presence of a strong emission at Br $\gamma$  in both components with different equivalent width, makes this scenario unlikely. Overall, T Tau Sb appears to be a regular T Tauri star, showing a photospheric spectrum and, additionally, strong accretion signatures such as a large Br $\gamma$  emission, and

significant veiling ( $r_K \approx 2$ ). Although significant emission in the hydrogen line can arise from chromospheric emission in M-type dwarfs (e.g., Martín 1998), we note that the equivalent width of the Br $\gamma$  line is very strong in T Tau Sb: only  $\sim 15\%$  of the classical T Tauri stars in Taurus studied by Muzerolle et al. (1998) show larger equivalent widths. Therefore we believe that emission in this line results from the usual T Tauri activity mechanisms.

The only unusual property of this object might well be its apparent faintness, which suggests that the extinction along the line of sight to T Tau Sb is fairly large. Its  $H - K$  color index, obtained by combining our relative photometry with the relatively stable absolute photometry for T Tau N from Kenyon & Hartmann (1995;  $K = 5.56$  and  $H = 6.36$ ), is about  $1.9 \pm 0.3$  mag. This is much redder than expected for a M1 dwarf ( $H - K \sim 0.2$  mag) and probably is the result of a combination of extinction and wavelength-dependent infrared excess related to the accretion phenomenon. Since its spectrum reveals photospheric features, it is possible to get a lower limit to the actual extinction towards this object by assuming that the continuum excess detected in the  $K$ -band does not extend into the  $H$ -band, where we would detect only photospheric flux. Since the photospheric flux from the star at  $K$  is only one third of the total flux, the excess-corrected color index of T Tau Sb is  $H - K \geq 0.7$  mag. The remaining color excess,  $\Delta(H - K) \geq 0.5$  mag, corresponds to an extinction along the line of sight of  $A_V \geq 8$  mag (Rieke & Lebofsky 1985), which is much larger than the extinction to T Tau N. Combining this with the intrinsic  $V - K$  color of a M1 dwarf ( $V - K = 3.8$  Kenyon & Hartmann 1995), we estimate that the expected visible magnitude of T Tau Sb is  $V > 19.7$ , which explains its non-detection by Gorham et al. (1992) and Stapelfeldt et al. (1998).

#### 4.2. Orbital motion within the triple system T Tau

As can be seen from Fig. 3, T Tau Sb is moving very fast with respect to T Tau Sa ( $4.2 \text{ AU yr}^{-1}$ , or  $20 \text{ km s}^{-1}$ , based on the latest two measurements). There are two potential explanations to this: either constant linear motion of a background star or orbital motion. We first consider the former possibility by comparing the observed motion to what is expected for a field star and show that they are unlikely to match each other.

First of all, one can extrapolate the expected location of a chance alignment background star at the time of the first epoch from the last two measurements, which are the most accurate. The predicted separation and position angle for December 1997 are  $0''.082 \pm 0.023$  and  $200 \pm 15^\circ$ . This is only  $1.5\sigma$  different from the measurement of Koresko (2000), which is not enough to exclude a constant linear motion of T Tau Sb with respect to T Tau Sa. If T Tau Sb was a background star, its velocity should be the sum of the proper motion of

T Tau N, which was measured by Jones & Herbig (1979), and the relative motion of the T Tau N/T Tau S pair, which has been estimated by Roddier et al. (2000). This combined motion, however, is about twice as slow as the observed motion and its direction is about forty degrees away. We thus conclude that T Tau Sb is not a background star. This is strongly reinforced by the extremely low probability,  $\sim 10^{-7}$  based on the  $2.5 \times 10^{-6}$  per square arcsecond surface density of objects brighter than  $K = 9$  estimated by the 2MASS survey around T Tau, of finding a star as bright as T Tau Sb within  $0''.1$  of T Tau Sa. Since T Tau Sb appears to be a normal T Tauri star, it probably belongs to the Taurus star-forming region, and we should compare its observed motion to the internal velocity dispersion in the molecular cloud, which is only  $2 \text{ km s}^{-1}$  (Jones & Herbig 1979; Hartmann et al. 1986). This is ten times smaller than what is observed, and it thus seems unlikely that this binary results from the visual alignment of two unrelated T Tauri stars.

Another serious issue for the scenario of a linear, independent motion of the two T Tau S components is the result of the lunar occultation observations presented by Simon et al. (1996), who failed to detect any companion to T Tau S. At the time of their observations, in December 1994, T Tau Sb should have been located  $\sim 0''.15$  away from T Tau Sa if its motion remained constant at the current observed speed. Although their observations would have failed to detect a companion in the same configuration as seen by Koresko (2000), such a large system would have been easy to detect unless it was then much fainter than it is currently (M. Simon, priv. comm.). Together with the relative speed of T Tau Sb, this suggests that the two stars form a bound system and that, for several years prior to its discovery, T Tau Sb was much closer to T Tau Sa than it is now.

We now assume that the observed motion is indeed that of a bound binary system, since it is statistically unlikely that we are witnessing an unstable triple system at the very moment of its disruption. Although three measurements are not enough to fit a complete orbital solution, one can still estimate the total mass of the system from an order of magnitude calculation. Fig. 3 obviously indicates that the observed motion cannot be a face-on circular orbit: the orbit must be inclined and/or eccentric. Assuming a 15 AU-radius inclined circular orbit, which is one of the simplest possible fits, the observed velocity implies a total system mass of  $5 \pm 2 M_{\odot}$ , to be compared to the  $2 M_{\odot}$  mass of T Tau N (e.g., Koresko et al. 1997), and an orbital period of  $25 \pm 5 \text{ yrs}^4$ . Such a mass for the T Tau S pair implies a total mass of  $\sim 7 M_{\odot}$  for T Tau, a factor of two larger than a previous estimate by Roddier et al. (2000) on the basis of the wide pair orbital motion (estimated orbital period  $\approx 500 \text{ yr}$ ). However,

---

<sup>4</sup>Only the uncertainty on the velocity is propagated to estimate errors here. We caution that the shape of the orbit is not constrained enough at this point and that these uncertainties should not be considered as absolute.

this mismatch is not statistically significant, as the dependency of orbital velocities to mass is only a square root effect and the measured velocities are fairly small. Independent of the details of the orbital motion within T Tau S, we can reasonably assume that its orbital period is on the order of a few decades. This implies that T Tau, considered as a triple system is gravitationally stable since the ratio of the orbital periods involved is at least a factor of ten (Eggleton & Kiseleva 1995).

The presence of a third component in the system might bias attempts to reconstruct the orbital motion of the wide T Tau N/T Tau S pair, as the orbital motion of T Tau S would result in a shift of its photocenter, which was used in previous studies of the system. However, using gaussian profiles to model both components of T Tau S, one can show that the photocenter should not move away from T Tau Sa by more than  $0''.005$  *if* T Tau Sb does not get much brighter than it currently is. Under this assumption, which is unverified in the long run, the observed motion of the unresolved T Tau S pair mostly relates to its orbit with T Tau N.

### 4.3. Geometry of the system

Our study confirms that T Tau S is a tight binary system and further shows that T Tau Sb is a strongly extincted early M-type T Tauri star, quite different from T Tau Sa which is now identified as the actual IRC. This allows us to revisit the various explanations proposed so far about the physical nature of the later object. We start by investigating the geometry of the system, before we move on to the very nature of the IRC.

One of the most popular theories to account for the properties of T Tau S, first suggested by Hogerheijde et al. (1997), is that it lies behind the optically thick circumstellar disk surrounding T Tau N. We know that this disk is likely seen close to face-on, as both the analysis of rotation properties of T Tau N and velocity measurements of the collimated outflow from that star suggest that its polar axis is only inclined by about  $20^\circ$  to the line of sight (Eisloffel & Mundt 1998). To prevent disk truncation by gravitational resonances, the actual separation of the wide pair must be much larger than the disk itself (cf., Lin & Papaloizou 1993). This implies that the T Tau N disk and T Tau N–T Tau S orbit are not coplanar, with T Tau S currently lying well beyond the disk. Therefore, the two components of T Tau S are likely to suffer roughly from the same extinction. Yet, the featureless spectrum of T Tau Sa contrast sharply with the numerous photospheric lines identified in that of T Tau Sb, which suggests that the disk of T Tau N, even though it may lie between us and T Tau S, is not the only factor responsible for the unusual characteristics of the IRC, unless the disk around T Tau N is very clumpy on a few AU scale. We conclude that T Tau S is surrounded by some optically thick material located much closer to the stars than T Tau N

and its disk are, as pointed out by the accretion diagnoses found in the spectrum of T Tau Sb which are suggestive of a circumstellar disk.

This analysis suggests that T Tau Sa is deeply embedded in a substantial amount of dusty material which reprocesses photons at mid-infrared wavelengths and annihilates any near-infrared photospheric feature. Alternatively, T Tau Sa could be intrinsically featureless, either because it is an F star, but such strong hydrogen emission lines and red colors have never been found in young intermediate-mass stars, or because its spectrum is completely dominated by an accretion-induced continuum flux. Even if the absence of photospheric features is not due to photon reprocessing by dust grains, the extinction towards T Tau Sa has to be very large to account for its non-detection in the visible, probably much larger than that towards T Tau Sb<sup>5</sup>. Although the T Tau S binary might be surrounded by a significant circumbinary envelope, the independent variability of both components suggests that they both have their own circumstellar obscuring material, which can be an almost edge-on disk or a more spherical thick envelope. In any case, this material must be confined to within a few AUs of each star, as orbital motion of the close pair would have truncated them long ago otherwise. These structures must be fed from an envelope surrounding the whole system in order to avoid complete clearance within a few thousands years: the extinction-corrected Br $\gamma$  flux from T Tau Sb only,  $F_{Br\gamma}(\text{T Tau Sb}) \geq 8.5 \cdot 10^{-14} \text{ erg.cm}^{-2}.\text{s}^{-1}$ , implies an accretion rate of  $\dot{M} \geq 10^{-8} M_{\odot}.\text{yr}^{-1}$  on that component (Muzerolle et al. 1998), while the non-detection of thermal emission from T Tau S by Akeson et al. (1998) places an upper limit of about  $7 \times 10^{-4} M_{\odot}$  on the mass of the gaseous material surrounding the tight binary. The existence of such a vast envelope was suggested by Hogerheijde et al. (1997) to fit the mid- to far-infrared unresolved flux of the system, and it could also account for the past variability of T Tau N (Beck & Simon 2001).

Overall, our study does not dramatically modify the geometry depicted by Solf & Böhm (1999) from their analysis of the two outflows known in this system, that is T Tau N seen pole-on in the foreground of T Tau S which is close to edge-on. However, we believe that the disk of T Tau N does not heavily obscure T Tau S. On the other hand, both T Tau Sa and T Tau Sb possess their own obscuring circumstellar material. The orientation of the jet emanating from T Tau S, almost in the plane of the sky, suggests that the star responsible for its launching could be seen through an almost edge-on disk. It is even possible that both circumstellar disks are parallel and seen almost edge-on, accounting for heavy extinction towards both components. In any case, the presence of accretion diagnostics in the spectra

---

<sup>5</sup>A visual extinction of  $A_V \approx 17.4 \text{ mag}$  has been derived by van den Ancker et al. (1999) on the basis of the depth of the silicate feature towards T Tau S. Given the flux ratio of the tight binary, this extinction applies to T Tau Sa.

of both components of T Tau S implies that they are both actively accreting, and hence that they are very likely surrounded by circumstellar disks. Whether we are looking at the stars through these disks or at higher inclination cannot be solved without much higher angular resolution studies allowed by techniques such as long-baseline interferometry. Finally, we emphasize that the presence of two stellar objects in the T Tau S system provides a natural explanation to the non-detection of thermal flux at millimeter wavelengths (Hogerheijde et al. 1997; Akeson et al. 1998), as discussed by Koresko (2000); most of the flux at these wavelengths normally comes from cold material located tens of AU away from the central star, but such material is likely to have been swept away by the orbital motion of the binary.

T Tau S has long been known to be the origin of non-thermal radio emission longwards of  $\lambda \sim 2$  cm (Phillips et al. 1993). This is thought to be the result of free-free emission either in an active magnetosphere or in an outflow. Recent high-angular resolution 2 cm observations of the T Tau system reveals that T Tau Sb is likely to be the source of this emission (K. Johnston *et al.* 2001, in preparation). This may suggest that T Tau Sb is the source of the outflow identified by Bohm & Solf (1994) from this system. On the other hand, if T Tau Sa is an accretion-dominated pre-main sequence object (Fu Ori-like), as first suggested by Ghez et al. (1991), it is also likely to drive a significant bipolar jet, as most of the younger, class I objects do; in that picture T Tau Sb could be the source of magnetospheric free-free radio emission while the optical jet would originate from T Tau Sa. It is thus still unclear which of the two components drives the outflow known to originate in the unresolved binary.

#### 4.4. On the nature of the IRC phenomenon

The spectrum of T Tau Sb reveals that it is a normal T Tauri star that is strongly extincted, likely due to the presence of some circumstellar/binary envelope (see above). On the other hand, the exact nature of T Tau Sa remains unclear. The mystery surrounding the IRC T Tau S has just been shifted towards its brightest component in the near-infrared. This could be an intermediate-mass star (spectral type F or so), an accretion-dominated object or a simple T Tauri star suffering a moderate accretion rate. In any case, it is deeply embedded into some sort of circumstellar material, which is confined into a volume of a few AU in radius, at most. Although this material could form a passive circumstellar envelope, a significant accretion rate on T Tau Sa is evidenced by the strong Br $\gamma$  emission line in its spectrum. Furthermore, the variability of this object cannot be simply explained by extinction changes, so that it has to be related to some intrinsic variability (van den Ancker et al. 1999). The most likely explanation is that the accretion-induced luminosity dominates the total flux of the object and varies with time, reinforcing the FU Ori-like model.

The total mass estimated for the T Tau S system from the observed orbital motion (§ 4.2) suggests that T Tau Sa is quite massive, as T Tau Sb is an early M-type star, and therefore is likely to be on the order of only  $M \approx 0.5 M_{\odot}$ . Although the mass of T Tau Sa remains uncertain, it is likely to be at least as massive as T Tau N. If it really is the most massive star in the system, the peculiarity of the IRC could be a direct consequence of its mass, as already suggested by Koresko et al. (1997). Because of its deeper potential well, the IRC could both retain a much denser circumstellar envelope than its neighbours and concentrate most of the feeding material coming from the vast reservoir surrounding the whole system, thus accounting for its apparent properties. We note however that, if it is not itself a tight binary consisting of two  $\sim 2 M_{\odot}$  objects, a mass much larger than  $3 M_{\odot}$  for T Tau Sa is problematic for several reasons: even though T Tau is among the youngest T Tauri systems (0.6 Myr, Koresko et al. 1997), a  $4 M_{\odot}$  is already an early-A or late-B star and it is already close to or on the main sequence at this age. Its luminosity would then be in the range 100–1000  $L_{\odot}$ , which is much larger than the bolometric luminosity of T Tau S (Koresko et al. 1997). Furthermore, such a hot star would create a very strong radiative pressure field and would likely blow away the surrounding dusty envelope. Either the system is not coeval, with T Tau Sa in an earlier evolutionary stage, or the mass of this star is currently overestimated. A continued follow-up of the T Tau Sa/T Tau Sb orbit over the next few years will help to refine the orbital parameters.

## 5. Conclusion

We obtained new  $H$  and  $K$  images of the T Tau triple system with the adaptive optics system at the 10 m Keck telescope, as well as the first resolved medium-resolution ( $R \sim 3500$ )  $K$ -band spectra of the two components of T Tau S, identified so far as an IRC to T Tau N. Our data reveal that T Tau Sb is a heavily extincted, actively accreting M1 pre-main sequence object, i.e. a rather normal T Tauri star. On the other hand, T Tau Sa, which dominates the system in the near-infrared, is indeed identified as the IRC: its spectrum shows no feature except for a significant  $\text{Br}\gamma$  emission line. Unlike previous observations, we do not detect the  $2.12 \mu\text{m}$   $\text{H}_2$  emission line in either of the two components.

The tight T Tau S binary shows significant motion since its first detection, almost three years prior to our observations. Although it is not yet inconsistent with a constant linear motion, it seems quite unlikely that this is because either one of the two objects is a background object, since they both show strong signs of T Tauri-like activity. Interpreting the observed motion as that of two stars orbiting each other, and assuming that the orbit is inclined and circular, we derive rough estimates for the orbital parameters. The total system

mass and orbital periods are on the order of  $5 M_{\odot}$  and 25 yrs, although we emphasize that the uncertainty on the actual orbit shape is not taken into account here.

Although T Tau S might well be located behind the circumstellar disk of T Tau N, we argue here that this is *not* the main reason for the peculiarities of T Tau S, because of the strikingly different properties of T Tau Sa, which is now identified as the IRC, and T Tau Sb as well as from an analysis of the optical depth of the circumprimary disk. Both components of T Tau S are likely embedded in their own circumstellar material, which could be either an almost edge-on disk or a dense spheroidal envelope. Because of tidal truncation due to the tight binary’s orbit, this material must be confined to within only a few AU of the stars, making it too small to be resolved by current observations. Furthermore, this effect also explains the non-detection of thermal flux in the radio domain, as most of the material located in the corresponding range of distance from the stars has been swept away. In any event, the subsistence of dense envelopes on a few AU scale around both components of T Tau S for several  $10^5$  yrs requires that they are being replenished by material coming from a larger scale reservoir such as a vast envelope surrounding the whole system. The presence of such a structure was already suspected from the analysis of the spectral energy distribution from the system.

Following the orbit of T Tau S for a few more years will bring a definitive conclusion regarding the possibility that the system is simply a projected, unphysical one and provide a much better estimate of the orbit shape and parameters if the two stars are bound. Furthermore, high-spectral resolution data will yield radial velocities, which are very powerful tools to better constrain the orbit, and potentially reveal for the first time some photospheric features, which would greatly help understanding the nature of this peculiar object. We also note that both components of T Tau S are prime targets for the upcoming long-baseline interferometry experiments, as the environment of these stars can only be resolved through these techniques.

Data presented herein were obtained at the W. M. Keck Observatory, which is operated as a scientific partnership among the California Institute of Technology, the University of California and the National Aeronautics and Space Administration. The Observatory was made possible by the generous financial support of the W. M. Keck Foundation. The Observatory staff supported our observations very efficiently and we wish to thank them, more particularly Joel Aycock, David Le Mignant and David Sprayberry. We also thank Bruce Macintosh for his help during the observations and Franck Marchis for providing us with synthetic point spread functions used to estimate Strehl ratios in our images. We acknowledge our anonymous referee for his prompt and helpful report, as well as Michal Simon for extensive discussions about T Tau S and valuable comments on an early version of this

paper. This work has been supported in part by the National Science Foundation Science and Technology Center for Adaptive Optics, managed by the University of California at Santa Cruz under cooperative agreement No. AST-9876783, by NASA’s Origins of Solar System program grant No. NAG-6975 and by the Packard Foundation. This research makes use of the SIMBAD database, operated at CDS, Strasbourg, France, and of data products from the Two Micron All Sky Survey, which is a joint project of the University of Massachusetts and the Infrared Processing and Analysis Center/California Institute of Technology, funded by the National Aeronautics and Space Administration and the National Science Foundation. The authors wish to extend special thanks to those of Hawaiian ancestry on whose sacred mountains we are privileged to be guests. Without their generous hospitality, none of the observations presented herein would have been possible.

## REFERENCES

- Akeson, R. L., Koerner, D. W., & Jensen, E. L. N. 1998, *ApJ*, 505, 358
- Ali, B., Carr, J. S., Depoy, D. L., Frogel, J. A., & Sellgren, K. 1995, *AJ*, 110, 2415
- Beck, T. L. & Simon, M. 2001, *AJ*, 122, 413
- Beck, T. L., Prato, L., & Simon, M. 2001, *ApJ*, 551, 1031
- Bertout, C., Basri, G., & Bouvier, J. 1988, *A&A*, 330, 350
- Bohm, K.-H. & Solf, J. 1994, *ApJ*, 430, 277
- Cohen, M. & Kuhl, L. V. 1979, *ApJS*, 41, 743
- Dyck, H. M., Simon, T., & Zuckerman, B. 1982, *ApJ*, 255, L103
- Eggleton, P. & Kiseleva, L. 1995, *ApJ*, 455, 640
- Eisloffel, J. & Mundt, R. 1998, *AJ*, 115, 1554
- Elias, J. H. 1978, *ApJ*, 224, 857
- Ghez, A. M., Weinberger, A. J., Neugebauer, G., Matthews, K., & McCarthy, D. W. 1995, *AJ*, 110, 753
- Ghez, A. M., Neugebauer, G., & Matthews, K. 1993, *AJ*, 106, 2005
- Ghez, A. M., Neugebauer, G., Gorham, P. W., Haniff, C. A., Kulkarni, S. R., Matthews, K., Koresko, C., & Beckwith, S. 1991, *AJ*, 102, 2066

- Gorham, P. W., Ghez, A. M., Haniff, C. A., Kulkarni, S. R., Matthews, K., & Neugebauer, G. 1992, *AJ*, 103, 953
- Hanson, M. M., Conti, P. S., & Rieke, M. J. 1996, *ApJS*, 107, 281
- Hartmann, L., Hewett, R., Stahler, S., & Mathieu, R. D. 1986, *ApJ*, 309, 275
- Herbst, T. M., Beckwith, S. V. W., Glindemann, A., Tacconi-Garman, L. E., Kroker, H., & Krabbe, A. 1996, *AJ*, 111, 2403
- Hogerheijde, M. R., van Langevelde, H. J., Mundy, L. G., Blake, G. A., & van Dishoeck, E. F. 1997, *ApJ*, 490, L99
- Jones, B. F. & Herbig, G. H. 1979, *AJ*, 84, 1872
- Joy, A. H. 1945, *ApJ*, 102, 168
- Kenyon, S. J. & Hartmann, L. 1995, *ApJS*, 101, 117
- Kleinmann, S. G. & Hall, D. N. B. 1986, *ApJS*, 62, 501
- Kobayashi, N., Nagata, T., Hodapp, K., & Hora, J. L. 1994, *PASJ*, 46, L183
- Köhler, R., Kasper, M. & Herbst, T. 2000, *in* “Birth and evolution of binary stars”, poster proceedings of IAU symp. 200, eds. B. Reipurth & H. Zinnecker, p. 63
- Koresko, C. D. 2000, *ApJ*, 531, L147
- Koresko, C. D., Herbst, T. M., & Leinert, Ch. 1997, *ApJ*, 480, 741
- Leinert, Ch., Zinnecker, H., Weitzel, N., Christou, J., Ridgway, S. T., Jameson, R., Haas, M., & Lenzen, R. 1993, *A&A*, 278, 129
- Lin, D. N. C. & Papaloizou, J. C. B. 1993, *Protostars and Planets III*, 749
- Martín, E. L. 1998, *AJ*, 115, 351
- McLean, I. S., Graham, J. R., Becklin, E. E., Figer, D. F., Larkin, J. E., Levenson, N. A., & Teplitz, H. I. 2000, *Proc. SPIE*, 4008, 1048
- Muzerolle, J., Hartmann, L., & Calvet, N. 1998, *AJ*, 116, 2965
- Phillips, R. B., Lonsdale, C. J., & Feigelson, E. D. 1993, *ApJ*, 403, L43
- Rieke, G. H. & Lebofsky, M. J. 1985, *ApJ*, 288, 618

- Roddier, F., Roddier, C., Brandner W., Charissoux, D., Véran, J.-P., & Courbin, F. 2000, *in* “Birth and evolution of binary stars”, poster proceedings of IAU symp. 200, eds. B. Reipurth & H. Zinnecker, p. 60
- Simon, M., Longmore, A. J., Shure, M. A., & Smillie, A. 1996, *ApJ*, 456, L41
- Simon, M., Ghez, A. M., Leinert, Ch., Cassar, L., Chen, W. P., Howell, R. R., Jameson, R. F., Matthews, K., Neugebauer, G., & Richichi, A. 1995, *ApJ*, 443, 625
- Solf, J. & Böhm, K.-H. 1999, *ApJ*, 523, 709
- Stapelfeldt, K. R., Burrows, C. J., Krist, J. E., Watson, A. M., Ballester, G. E., Clarke, J. T., Crisp, D., Evans, R. W., Gallagher, J. S. III, Griffiths, R. E., Hester, J. J., Hoessel, J. G., Holtzman, J. A., Mould, J. R., Scowen, P. A., Trauger, J. T., Westphal, J. A. 1998, *ApJ*, 508, 736
- Van Cleve, J. E., Hayward, T. L., Houck, J. R., & Miles, J. 1994, American Astronomical Society Meeting, 184, 4405
- van den Ancker, M. E., Wesselius, P. R., Tielens, A. G. G. M., van Dishoeck, E. F., & Spinoglio, L. 1999, *A&A*, 348, 877
- van Langevelde, H. J., van Dishoeck, E. F., van der Werf, P. P., & Blake, G. A. 1994, *A&A*, 287, L25
- Wallace, L. & Hinkle, K. 1997, *ApJS*, 111, 445
- Wizinowich, P. L., Acton, D. S., Lai, O., Gathright, J., Lupton, W., & Stomski, P. J. 2000, *Proc. SPIE*, 4007, 2

Table 1: Astrometric and relative photometric results

Binary	Relative astrometry		Relative photometry	
	sepn.	P.A. <sup>a</sup>	$\Delta K$ (mag)	$\Delta H$ (mag)
Sa–Sb	$0''.092 \pm 0''.003$	$267.0 \pm 1.6$	$1.89 \pm 0.05$	$1.17 \pm 0.02$
N–Sa	$0''.702 \pm 0''.005$	$179.7 \pm 0.2$	$1.36 \pm 0.05$	$3.17 \pm 0.02$
N– <i>Stot</i> <sup>b</sup>			$1.18 \pm 0.03$	$2.87 \pm 0.02$

<sup>a</sup>Position angles are measured Eastwards from North.

<sup>b</sup>*Stot* stands for the unresolved T Tau S pair.

Table 2: Spectral results<sup>a</sup>

Object	S.T.	EW Br $\gamma$ (Å)	EW H <sub>2</sub> (Å)
Sa	–	$3.8 \pm 0.2$	$< 0.5$
Sb	M1	$6.5 \pm 0.2$	$< 0.5$
N	K1 <sup>b</sup>	$3.0 \pm 0.2^c$	$< 0.6^c$

<sup>a</sup>The equivalent widths of the Br $\gamma$  and H<sub>2</sub> 2.12  $\mu$ m lines measure their strength in emission or  $3\sigma$  upper limits for those which were not detected.

<sup>b</sup>from Cohen & Kuhi (1979)

<sup>c</sup>from Beck et al. (2001)

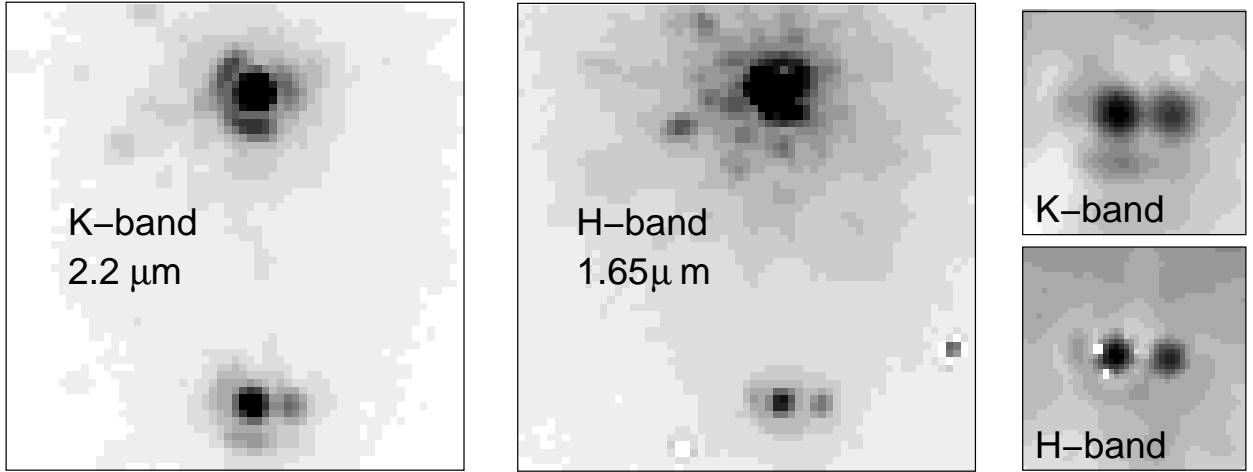


Fig. 1.— *Left and center:* *K*- and *H*-band images of the whole T Tau system. A square-root stretch was used to allow a proper identification of all components of the system; T Tau N dominates the system at both wavelengths. North is up, and East to the left. Both images are approximately  $1''$  on each side and T Tau Sb is located just West of T Tau Sa. In spite of the increased brightness of both T Tau S components at longer wavelength, the two are best resolved in the *H*-band image. *Right:* Images of T Tau S lightly deconvolved with a Lucy-Richardson algorithm using T Tau N as the empirical point spread function. The images have been resampled by a factor of two in both directions and the image size is about  $0''.4$ .

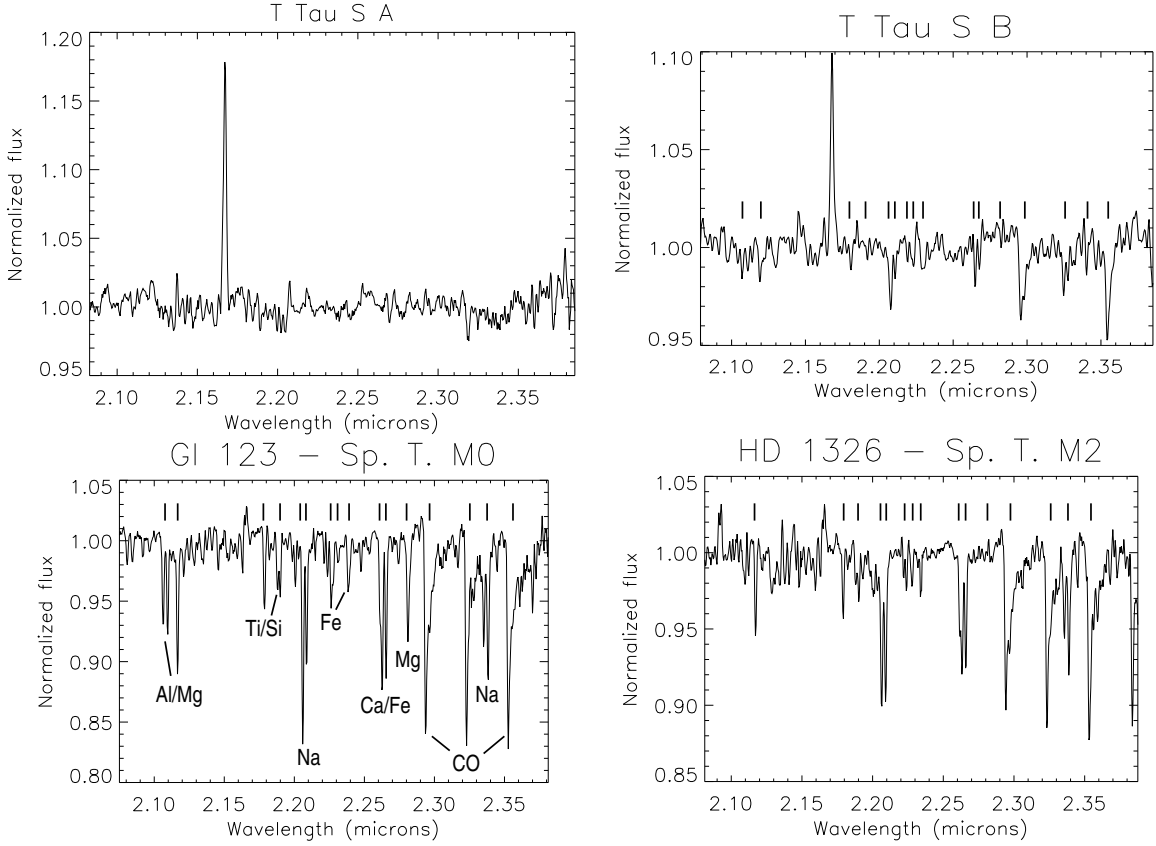


Fig. 2.— *K*-band spectra of T Tau Sa (upper left) and T Tau Sb (upper right), compared to M0 and M2 dwarfs observed during the same run (lower left and right spectra, respectively). All spectra were convolved to a final resolution of  $R \sim 1500$  to increase the signal-to-noise ratio and normalized to a low-order polynomial continuum. Note the different vertical scale for each spectrum. The T Tau Sa spectrum was corrected for atmospheric absorption using HR 1388 as a calibrator, while the T Tau Sb spectrum was divided by the (featureless) spectrum of T Tau Sa (see text). All features used for spectra typing are marked in the spectra of T Tau Sb and the dwarf standards and are identified in the spectrum of Gl 123 for comparison.

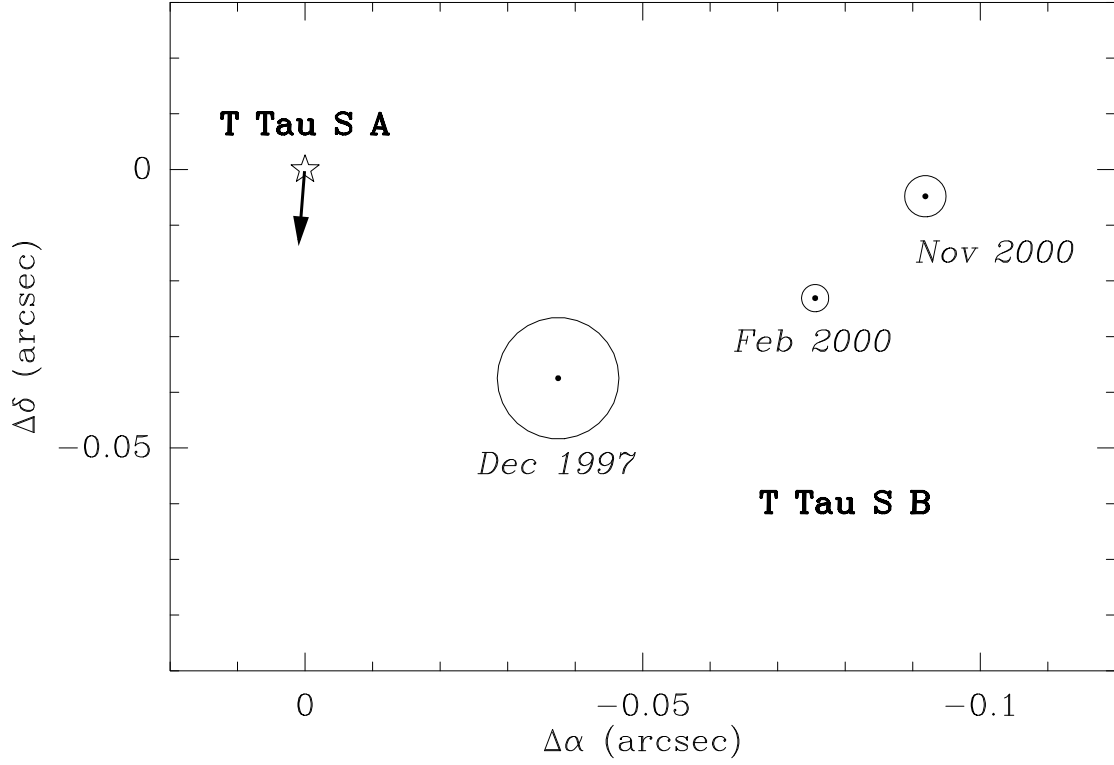


Fig. 3.— Motion of T Tau Sb with respect to T Tau Sa. The large circles represent the  $1\sigma$  uncertainties of the three detections of the binary to date (Koresko 2000; Köhler et al. 2000, and this paper). The arrow represents the expected proper motion per year of T Tau Sa with respect to background stars, which is assumed to be the sum of that of T Tau N and the orbital motion of the wide pair (see text for details).